

# Contrasting patterns of Bim induction and neuroprotection in Bim-deficient mice between hippocampus and neocortex after *status epilepticus*

BM Murphy<sup>1</sup>, T Engel<sup>1</sup>, A Paucard<sup>1</sup>, S Hatazaki<sup>1,2</sup>, G Mouri<sup>1,2</sup>, K Tanaka<sup>1,2</sup>, LP Tuffy<sup>1</sup>, EM Jimenez-Mateos<sup>1</sup>, I Woods<sup>1</sup>, M Dunleavy<sup>1</sup>, HP Bonner<sup>1</sup>, R Meller<sup>3</sup>, RP Simon<sup>3</sup>, A Strasser<sup>4</sup>, JHM Prehn<sup>1</sup> and DC Henshall<sup>\*,1</sup>

Prolonged seizures (*status epilepticus*) are associated with brain region-specific regulation of apoptosis-associated signaling pathways. Bcl-2 homology domain 3-only (BH3) members of the Bcl-2 gene family are of interest as possible initiators of mitochondrial dysfunction and release of apoptogenic molecules after seizures. Previously, we showed that expression of the BH3-only protein, Bcl-2 interacting mediator of cell death (Bim), increased in the rat hippocampus but not in the neocortex after focal-onset *status epilepticus*. In this study, we examined Bim expression in mice and compared seizure damage between wild-type and Bim-deficient animals. *Status epilepticus* induced by intra-amygdala kainic acid (KA) caused extensive neuronal death within the ipsilateral hippocampal CA3 region. Hippocampal activation of factors associated with transcriptional and posttranslational activation of Bim, such as CHOP and c-Jun NH(2)-terminal kinases, was significant within 1 h. Upregulation of *bim* mRNA was evident after 2 h and Bim protein increased between 4 and 24 h. Hippocampal CA3 neurodegeneration was reduced in Bim-deficient mice compared with wild-type animals after seizures *in vivo*, and short interfering RNA molecules targeting *bim* reduced cell death after KA treatment of hippocampal organotypic cultures. In contrast, neocortical Bim expression declined after *status epilepticus*, and neocortex damage in Bim-deficient mice was comparable with that in wild-type animals. These results show region-specific differential contributions of Bim to seizure-induced neuronal death.

*Cell Death and Differentiation* (2010) 17, 459–468; doi:10.1038/cdd.2009.134; published online 25 September 2009

Signaling pathways associated with the orchestration of apoptosis may contribute to neuronal death after experimental seizures.<sup>1</sup> Both caspase-dependent and -independent apoptosis pathways have been implicated.<sup>1</sup> The Bcl-2 gene family members are critical upstream regulators of the mitochondrial (intrinsic) apoptotic pathway.<sup>2</sup> Prolonged seizures (*status epilepticus*) and glutamate excitotoxicity in certain models cause mitochondrial dysfunction and release of apoptogenic molecules, such as cytochrome *c*,<sup>3</sup> and apoptosis inducing factor (AIF).<sup>4</sup> Support for the involvement of Bcl-2 family members comes from several observations. Seizures cause multidomain proapoptotic Bax to cluster around mitochondria at the time of cytochrome *c* release,<sup>5</sup> and Bax-deficient neurons have been reported to be abnormally resistant to excitotoxicity.<sup>6</sup> Moreover, the overexpression of antiapoptotic Bcl-xL reduces cell death after seizure-like insults *in vivo*,<sup>7</sup> and conversely, mice deficient in antiapoptotic Bcl-w are abnormally vulnerable to hippocampal damage after seizures.<sup>3</sup> However, a functional role for Bax in excitotoxicity has been excluded by some studies.<sup>4</sup> Furthermore, calcium exposure of mitochondria alone<sup>8</sup> and calpain activity<sup>9</sup> can trigger the

release of apoptogenic factors from mitochondria in neurons independently of Bcl-2 family proteins.

Members of the Bcl-2 homology domain 3-only (BH3) subfamily are critical initiators of intrinsic apoptosis signaling and function by activating Bax/Bak either through direct binding or indirectly by binding and inhibiting antiapoptotic Bcl-2 family members.<sup>2</sup> The Bcl-2 interacting mediator of cell death (Bim) is among the most potent of BH3-only proteins, because, unlike some BH3-only proteins (e.g., Bad), it avidly binds all antiapoptotic Bcl-2 members.<sup>10</sup> The expression of Bim is detectable at low levels in normal (unstressed) brain.<sup>11</sup> Bim expression is controlled by a complex series of transcription factors, such as forkhead transcription factors belonging to the FoxO subfamily,<sup>12,13</sup> c-Jun<sup>14</sup> and CHOP (CCAAT/enhancer-binding protein-homologous protein, also known as GADD153).<sup>15</sup> Bim activity is also regulated posttranslationally. The c-Jun NH(2)-terminal kinases (JNK) can phosphorylate Bim and thereby potentiate its activity,<sup>16,17</sup> whereas phosphorylation by mitogen-activated protein kinases leads to Bim inactivation<sup>18</sup> and/or to ubiquitin-mediated degradation.<sup>19,20</sup> Bim-deficient cells are resistant

<sup>1</sup>Department of Physiology and Medical Physics, Royal College of Surgeons in Ireland, Dublin, Ireland; <sup>2</sup>Department of Neurosurgery, Mie University School of Medicine, Tsu, Mie, Japan; <sup>3</sup>Robert S Dow Neurobiology Laboratories, Legacy Research, Portland, OR, USA and <sup>4</sup>Molecular Genetics of Cancer Division, The Walter and Eliza Hall Institute of Medical Research, Melbourne, Australia

\*Corresponding author: DC Henshall, Department of Physiology and Medical Physics, Royal College of Surgeons in Ireland, 123 St. Stephen's Green, Dublin 2, Ireland. Tel: +353 1402 8629; Fax: +3531402 2447; E-mail: dhenshall@rcsi.ie

**Keywords:** apoptosis; Bax; Bcl-2; FKHR; JNK; temporal lobe epilepsy

**Abbreviations:** BH3, Bcl-2 homology domain 3-only; AIF, apoptosis inducing factor; Bim, Bcl-2 interacting mediator of cell death

Received 01.4.09; revised 03.8.09; accepted 19.8.09; Edited by RA Knight; published online 25.9.09

to certain apoptotic stimuli, including deregulated calcium flux,<sup>21</sup> and Bim has also been reported to function in caspase-independent pathways in neurons by stimulating AIF release.<sup>22</sup>

We previously demonstrated that Bim is rapidly induced in the rat hippocampus after focal-onset *status epilepticus*.<sup>23</sup> Bim levels were not altered in the neocortex, although Bim was downregulated after repeated brief, nondamaging seizures, a model of epileptic tolerance.<sup>23</sup> Using an *in vitro* model of seizure-like injury, Bim upregulation was linked to the FoxO1 transcription factor, and antisense targeting of *bim* mRNA reduced neuronal death.<sup>23</sup> Despite these findings, the relationship between seizures, Bim activation and regional vulnerability remains uncertain, and a causal role *in vivo* remains unproven. In this study, we used a combination of *in vivo* and *in vitro* mouse models and cells deficient in or depleted of Bim to characterize the expressional response of Bim and to determine whether Bim is important for seizure-induced neuronal death.

## Results

**Hippocampal seizures and subfield-specific damage after focal-onset *status epilepticus*.** To examine the role of Bim during seizure-induced neuronal death, we used a model of focal-onset *status epilepticus* induced by an intra-amygdala microinjection of the glutamate analog kainic acid (KA), followed after 40 min by an injection of lorazepam to limit damage and mortality.<sup>24,25</sup> First, we performed *in vivo* intra-hippocampal depth electrode recordings from the ipsilateral CA3 subfield during seizures. These recordings confirmed that the intra-amygdala KA microinjection elicited high-amplitude and high-frequency electrographic seizure discharges within the hippocampus (Figure 1a). Next, we examined hippocampal injury using Fluoro-Jade B (Chemicon Europe Ltd, Chandler's Ford, UK) to stain degenerating neurons. Confirming previous reports,<sup>24,25</sup> there occurred hippocampal neuronal death 24 h after seizures, which particularly affected the ipsilateral CA3 and hilar region (Figure 1b). In addition, minor and variable neuronal death was found in the CA1 subfield, as previously observed.<sup>24</sup> No neuronal death was observed in the hippocampus from vehicle-injected control mice (Figure 1b) or in the contralateral hippocampus of mice that underwent *status epilepticus* (data not shown).

**Upregulation of Bim in the hippocampus after focal-onset *status epilepticus*.** Quantitative real-time PCR-determined seizures caused an early (2 h) increase in the hippocampal levels of *bim* mRNA, and these levels remained elevated until at least 8 h later (Figure 1c). Western blot analysis of extracts from the seizure-damaged hippocampus revealed a significant increase in Bim protein levels at 4 h, which continued to increase at later time points examined (8 h and 24 h) (Figure 1d and e). The molecular weight of the Bim band corresponded to the Bim<sub>EL</sub> isoform (~26 kDa).<sup>10,11</sup> Bim induction was dependent on mice experiencing high-amplitude, high-frequency polyspike seizure discharges, because hippocampal Bim levels at 24 h in mice injected

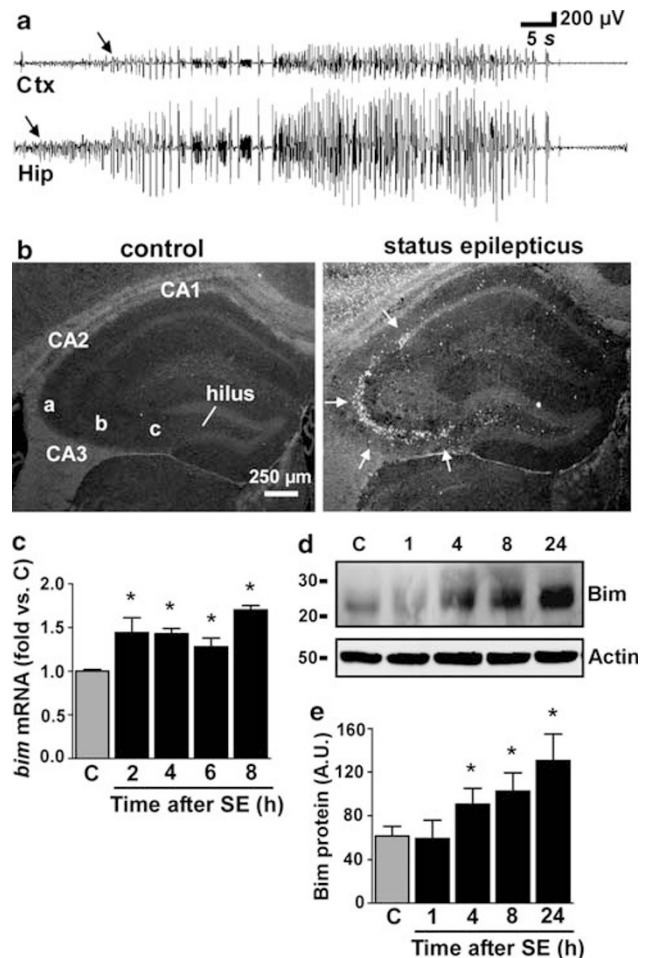


**Figure 1** Upregulation of Bim in the hippocampus during seizure-induced neuronal death. (a) Trace of a high-amplitude high-frequency seizure burst captured using combined intrahippocampal-cortical EEG. Arrows demark the point of onset. Note that seizure activity is detected in the hippocampus (Hip) before the cortex (Ctx). (b) Photomicrographs ( $4\times$  lens) show representative Fluoro-Jade B staining at 24 h in the Hip of control mice and in mice that underwent *status epilepticus* (SE). Arrows denote cells (white) undergoing degeneration. (c) Graph showing the quantification of mRNA levels for *bim* corrected to  $\beta$ -actin in control (C, 2 h) and in seizure-damaged mice at various time points after lorazepam was administered. Data are from four independent experiments. (d) Representative western blot ( $n=2$  per lane) showing increased expression of Bim 4–24 h after seizures compared with control and 1 h after seizure. Actin is shown as a control for protein loading. (e) Graph showing semiquantification of Bim protein levels. Data are from three independent experiments. AU, arbitrary units. Molecular weight markers are depicted to the left. \* $P<0.05$  compared with control

with KA that did not develop *status epilepticus* ( $n=2$ ) were similar to those seen in control brains (data not shown).

**Seizures activate FoxO transcription factors, CHOP and JNK, in hippocampus.** In an effort to determine the pathways involved in the upregulation of Bim in the hippocampus after seizures, we performed a western blot analysis of known transcription factors and modifiers of Bim activity. FoxOs and CHOP are known transcriptional

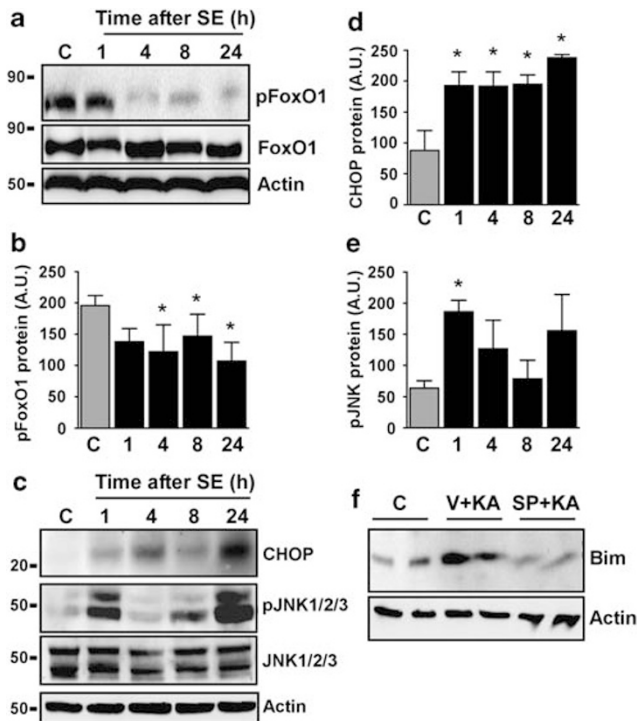


**Figure 2** Activation of transcription factors linked to Bim regulation in the hippocampus after status epilepticus. (a) Representative western blots ( $n=2$  per lane) showing that the expression of phosphorylated (p)FoxO1 declines after seizures. The blot below shows the nonphosphorylated form and actin as a protein loading control. (b) Graph showing the semiquantitative analysis of pFoxO1 levels in the hippocampus. (c) Representative western blots ( $n=2$  per lane) showing the expression of CHOP and JNK1/2/3 isoforms. Note the increased CHOP and pJNK levels. (d) Graph showing semiquantitative analysis of CHOP levels in the hippocampus. (e) Graph showing semiquantitative analysis of pJNK1/2/3. All graph data are from three independent experiments.  $*P<0.05$  compared with control (C, 4 h). (f) Representative western blots ( $n=1$  per lane) showing hippocampal Bim expression at 24 h in control and in KA-treated mice given either vehicle (V + KA) or JNK inhibitor SP600125 (SP + KA). Note the reduced Bim induction in seizure mice treated with SP600125. Actin is included as a protein loading control

inducers of *bim*.<sup>12,13,15,23</sup> Analysis of seizure-damaged mouse hippocampus revealed that levels of the inactive (phosphorylated) forms of FoxO1 and FoxO3 were significantly reduced after seizures (Figure 2a,b, data not shown). Somewhat preceding the FoxO response, the expression of CHOP was found to be significantly elevated within 1 h of seizures (Figure 2c and d). We next examined the phosphorylation (activation) state of the JNK/c-Jun pathway, which can directly upregulate *bim* mRNA or function posttranscriptionally to increase Bim activity by phosphorylation.<sup>14,16,17</sup> Phosphorylation of JNK1/2/3 in the hippocampus was significantly increased 1 h after seizures, returning to baseline thereafter (Figure 2c and e). No significant change was detected in total JNK1/2/3 protein levels (Figure 2c, data not shown).

**JNK inhibitor SP600125 prevents seizure-induced Bim upregulation.** To gain an insight into whether these pathways functionally contributed to Bim induction after

seizures, we examined the effect of blocking JNK *in vivo* using the specific inhibitor SP600125.<sup>26</sup> Bim expression was analyzed at 24 h in the ipsilateral hippocampus from control mice, as well as from KA-injected seizure mice given either intracerebroventricular vehicle or SP600125 (25  $\mu$ M) ( $n=4$  per group).

All vehicle- and SP600125-treated mice developed *status epilepticus* after KA, and seizure durations were not significantly different between groups (data not shown). As before, Bim expression was significantly increased in the hippocampus after seizures (to  $174 \pm 63\%$  of nonseizure control levels) (Figure 2f). In contrast, the induction of Bim was strongly reduced in seizure mice treated with SP600125 ( $125 \pm 45\%$  of control levels) (Figure 2f). SP600125 also blocked the induction of CHOP after *status epilepticus* (Supplementary Figure 1). Levels of pFoxO1 were not different between vehicle- and SP600125-treated mice 24 h after *status epilepticus* (data not shown).

**Bim expression declines in the neocortex after focal-onset *status epilepticus*.** We next analyzed cell death and Bim expression within the ipsilateral neocortex. In agreement with our previous report,<sup>25</sup> small numbers of degenerating neurons were found within the temporal, ectohippocampal, perirhinal and piriform cortex 24 h after *status epilepticus* (Figure 3a). The sparse cell death was mainly confined to cortical layers IV–VI, with layers I–III showing little or no cell death (Figure 3a). Thus, the neocortex represents a recruited brain region that undergoes less-extensive cell death compared with hippocampal CA3.

Western blot analysis of Bim in samples from the neocortex detected moderate levels of Bim in control mice (Figure 3b). In mice subjected to *status epilepticus*, cortical expression of Bim underwent a rapid and significant decline (Figure 3b).

We next examined the responses of transcriptional and posttranslational regulators of Bim expression. Phosphorylation of FoxO1 was largely unchanged in the neocortex after seizures (Figure 3c). Similarly, no increased CHOP was evident in the neocortex (Figure 3c). No change in the expression of phosphoJNK1/2/3 or total JNK1/2/3 was found at any time after seizures in the neocortex (Figure 3d).

To further explore the relationship between Bim regulation and cell death in the neocortex, we performed double-label fluorescence microscopy experiments on tissue sections. Bim immunoreactivity could be detected at low level in many cells in the control mouse neocortex (Figure 3e). A reduced Bim immunoreactivity was evident in the neocortex 24 h after *status epilepticus* (Figure 3e). Cells positive for DNA fragmentation detected by terminal deoxynucleotidyl transferase-mediated dUTP nick end labeling (TUNEL) showed minimal Bim immunoreactivity (Figure 3e).

**Normal brain architecture in Bim-deficient mice.** To determine whether Bim is required for seizure-induced neuronal death in either the hippocampus or the neocortex in this model, we compared seizure damage between wild-type (*bim*<sup>+/+</sup>) and Bim-deficient (*bim*<sup>-/-</sup>) mice. Representative genotyping of wild-type, heterozygous (*bim*<sup>+/-</sup>) and Bim-deficient mice is shown in Figure 4a. To examine whether *bim*<sup>-/-</sup> mice show any developmental abnormalities,

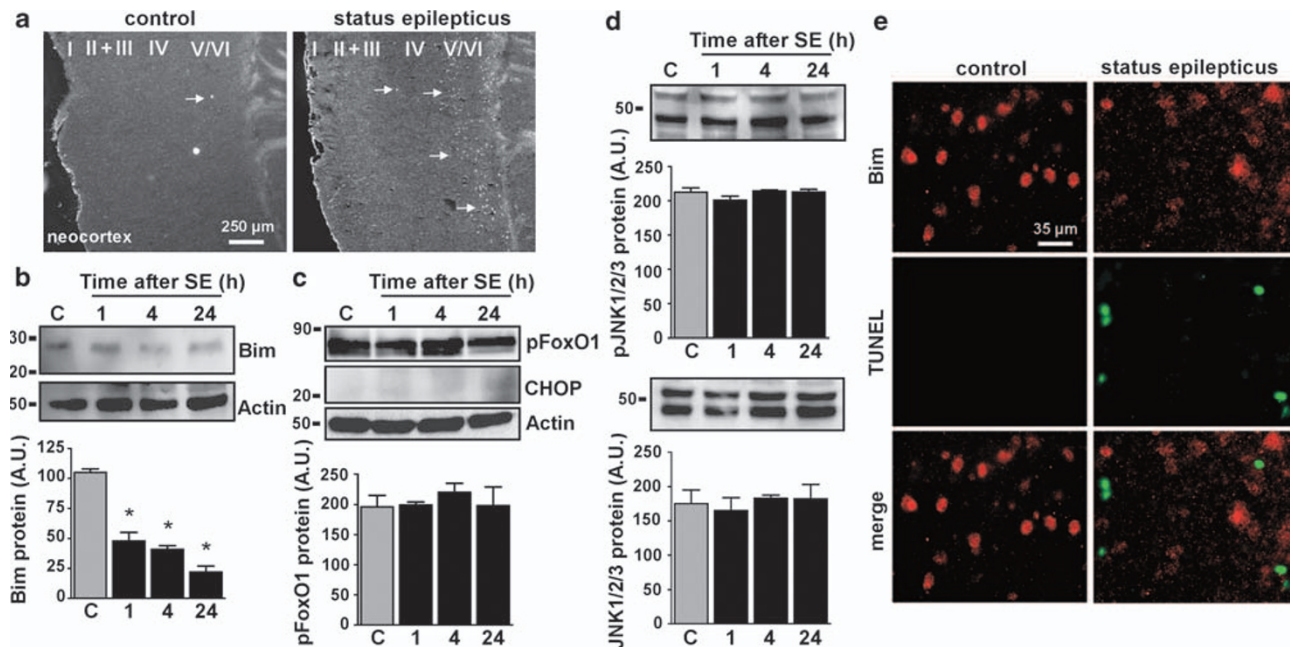


**Figure 3** Bim expression declines in the less-damaged neocortex after seizures. (a) Photomicrographs ( $4\times$  lens) show representative Fluoro-Jade B staining at 24 h in the neocortex of control mice and in mice that underwent *status epilepticus*. Arrows denote cells (white) undergoing degeneration. Cortical layers are indicated. (b) Representative western blot ( $n = 1$  per lane) showing decreased expression of Bim after seizures. Actin is shown as a control for protein loading. The graph below shows the semiquantification of Bim protein levels in the neocortex.  $*P < 0.05$  compared with control (C, 4 h). (c) Representative western blots ( $n = 1$  per lane) for pFoxO1, CHOP and actin and the corresponding semiquantification of protein levels for pFoxO1 in the neocortex. (d) Representative western blots ( $n = 1$  per lane) and graphs showing (top) pJNK1/2/3 and (bottom) total-JNK1/2/3 in the neocortex. All graph data are from three independent experiments. (e) Panels show representative  $40\times$  lens photomicrographs of Bim and TUNEL staining in the control and neocortex 24 h after *status epilepticus*. Note the decline in Bim staining and the presence of scattered TUNEL-positive cells after seizures

which might render them more or less prone to seizures or damage, we investigated the expression of KA receptor GluR6/7 in the amygdala (site of seizure elicitation) and a variety of genes in the hippocampus (site of major damage). Amygdala expression of GluR6/7 was not different between wild-type and *bim*<sup>-/-</sup> mice (Figure 4b). Similarly, the GluR6/7 expression in the hippocampus was comparable between both genotypes (Figure 4c). The hippocampal expression of Bad (another BH3-only protein) and Bcl-xL (an antiapoptotic Bcl-2 family member) was similar between both genotypes, although, as expected, Bim protein was not detected in brain lysates from *bim*<sup>-/-</sup> mice (Figure 4c). Moreover, under low- and high-power magnification, no gross hippocampal or cortical abnormalities were evident in *bim*<sup>-/-</sup> mouse brains (Figure 4d, data not shown). Counts of NeuN-stained hippocampal subfields from wild-type and *bim*<sup>-/-</sup> mice revealed similar numbers of neurons in all major hippocampal subfields—CA1, CA2 and CA3 (Figure 4e). Finally, we subjected groups of wild-type and *bim*<sup>-/-</sup> mice to seizures induced by intra-amygdala KA microinjection. Analysis of seizure EEG between injection and lorazepam administration confirmed no differences between the two genotypes of mice with respect to time-to-seizure onset, total duration of high-amplitude high-frequency bursts, the number of events recorded or duration of individual events (Figure 4f and data not shown). Taken together, these data confirm the suitability of *bim*<sup>-/-</sup> mice for analysis of seizure damage.

**Decreased hippocampal cell death in *bim*<sup>-/-</sup> mice compared with that in wild-type animals.** Fluoro-Jade B staining of tissue sections was performed 72 h after *status epilepticus*. This time point, rather than 24 h, was selected to ensure that any damage difference between wild-type and *bim*<sup>-/-</sup> animals was long lasting rather than transient. In wild-type mice, *status epilepticus* caused a typical lesion encompassing the ipsilateral CA3 subfield of the hippocampus (Figures 5a, c and e). In comparison, neurodegeneration after *status epilepticus* in *bim*<sup>-/-</sup> mice was ~45% less (Figures 5b, d and f). Counts of Fluoro-Jade B-positive cells in CA3 confirmed that there were significantly lower numbers of damaged/dying cells in *bim*<sup>-/-</sup> compared with wild-type animals (Figure 5g).

In contrast to the hippocampus, there was no significant difference in counts of Fluoro-Jade B-positive cells in the ipsilateral neocortex between wild-type and *bim*<sup>-/-</sup> mice (Figures 5h–j). Bim was also not required for KA-induced cortical neuron death *in vitro*, because cultures of primary cortical neurons from wild-type and Bim-deficient mice were similarly vulnerable to KA (Supplementary Figure 2).

**Bim knockdown is protective against KA-induced hippocampal cell death *in vitro*.** To support our *in vivo* data, we examined the role of Bim in neuronal death *in vitro* using a model of seizure-like injury to mouse organotypic hippocampal cultures.<sup>27</sup> In this model, KA ( $5\mu\text{M}$ ) treatment for 24 h results in neuronal death within the CA3 and CA1

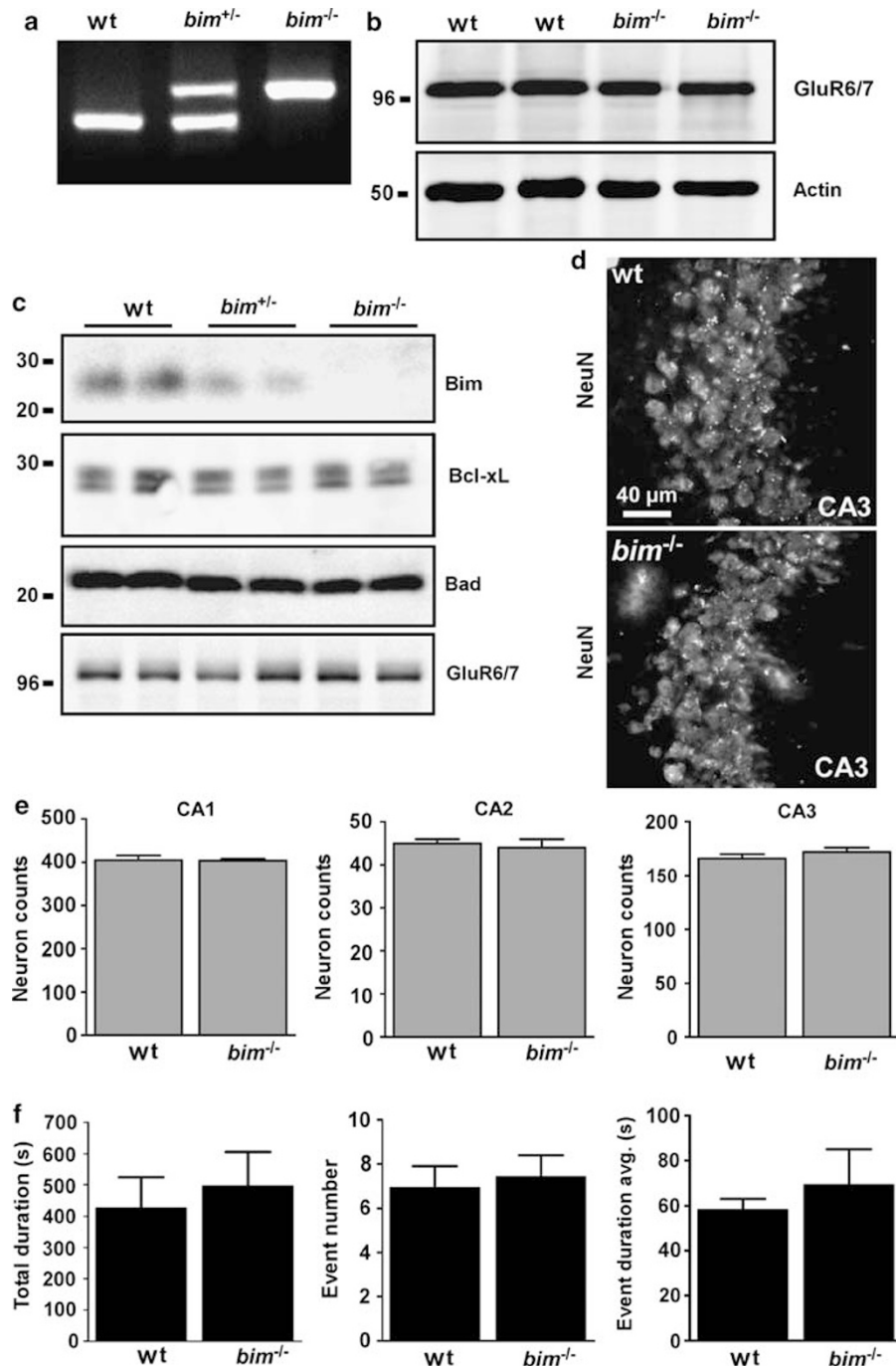


**Figure 4** Genotype and phenotype analysis of *bim*<sup>-/-</sup> mice. (a) Representative PCR showing genotyping of mice. (b) Representative western blot ( $n=2$  per lane) confirming normal expression of KA receptor GluR6/7 in the mouse amygdala between wild-type (wt) and *bim*<sup>-/-</sup> mice. Actin is shown as a control for protein loading. (c) Representative western blots of hippocampal samples confirming the absence of Bim protein in *bim*<sup>-/-</sup> mice, although the levels of a selection of other proteins are normal. (d) Representative photomicrographs of NeuN-stained CA3 subfields from wild-type and *bim*<sup>-/-</sup> mice. (e) Graphs showing counts of NeuN-positive cells in various hippocampal fields. No differences were evident between mice of the two genotypes ( $n=3$  per group). (f) Graphs showing EEG data on seizure parameters between wild-type and *bim*<sup>-/-</sup> mice after intra-amygdala KA microinjection. No differences were found between mice of the two genotypes ( $n=9-10$  per group)

subfields (Figures 6a, c, e and f). Western blot analysis of lysates from KA-treated hippocampal cultures revealed an increase in Bim expression levels compared with controls (Figure 6d). To determine whether Bim contributed to neuronal death in this model, we used a short interfering RNA (siRNA) approach to knock down Bim expression.

Hippocampal cultures were pretreated for 24 h with *bim*-targeting or nontargeting scrambled siRNA, and neuronal death was assessed 24 h after KA administration. Western blot analysis confirmed that siRNA targeting of *bim* reduced Bim protein expression after KA treatment (Figure 6d). In contrast, cultures treated with scrambled

siRNA showed a normal induction of Bim after KA administration (Figure 6d). As a further control, we verified that treatment of hippocampal cultures with siRNA had no significant effect on the expression of KA receptor GluR6/7 (Figure 6d). Analysis of cell death 24 h after KA revealed typical hippocampal CA1 and CA3 damage in cultures treated with scrambled siRNA (Figures 6b, c, e and f). In

contrast, hippocampal cultures treated with siRNA targeting *bim* showed significantly less cell death in both CA1 and CA3 when treated with KA, compared with KA-treated cultures treated with scrambled siRNA (Figures 6b, c, e and f).

## Discussion

The main findings of this study are the following: (1) focal-onset *status epilepticus* in mice is associated with a rapid induction of multiple transcription factors linked to *bim* regulation, as well as with an upregulation of *bim* mRNA and an increased expression of Bim protein in the hippocampus; (2) deficiency in Bim confers significant protection against hippocampal cell death after seizures *in vivo* and against KA-induced damage *in vitro*; and (3) Bim expression declines in the neocortex after seizures and this region is not protected in *bim*<sup>-/-</sup> mice. These studies demonstrate a differential and region-specific involvement of Bim in seizure-induced neuronal death, thereby providing a novel insight into gene-based mechanisms of seizure-induced neuronal death.

This study was undertaken to determine whether there is a causal role for Bim in seizure-induced neuronal death. Causal roles for Bim in neuronal death have previously been shown in models of neonatal hypoxia–ischemia,<sup>28</sup> and in motor neuron disease.<sup>29</sup> Functional roles for other Bcl-2 family members as killers or protectors in seizure-induced and excitotoxic neuronal death have been demonstrated, including for Bax or Bcl-xL and Bcl-w, respectively.<sup>3,6,7</sup> However, a requirement for Bcl-2 family members in mitochondrial dysfunction in these settings has been questioned by several reports. Excitotoxic neuronal death has been shown to occur normally in Bax-deficient neurons.<sup>4</sup> Furthermore, calcium exposure of mitochondria alone<sup>8</sup> and calpain activity<sup>9</sup> can trigger the release of apoptogenic factors from neuronal mitochondria. Functional redundancy among BH3-only proteins has been observed in various contexts.<sup>2</sup> The studies here provide evidence of Bim involvement in the molecular mechanism of seizure-induced neuronal death. The *in vivo* mouse model used is associated with neuronal death and with hallmarks of the intrinsic apoptosis pathway, such as cytochrome *c* release, caspase activation and double-stranded DNA fragmentation with nuclear clumping of fragmented chromatin in one-third of cells.<sup>3,24</sup> The data presented here show that Bim expression is increased at both mRNA and protein levels in injured hippocampus. The induction of Bim seems to be temporally compatible with a causal role in mitochondrial dysfunction because we have previously reported that cytochrome *c* is not

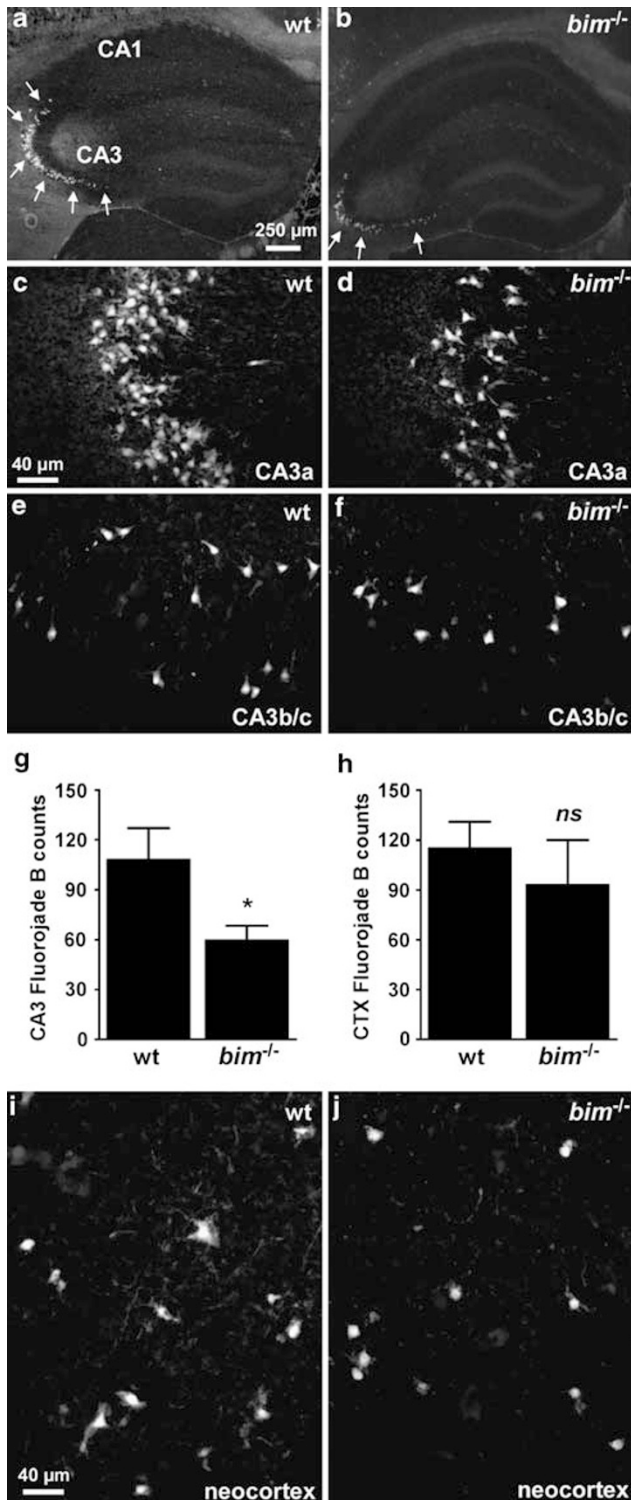
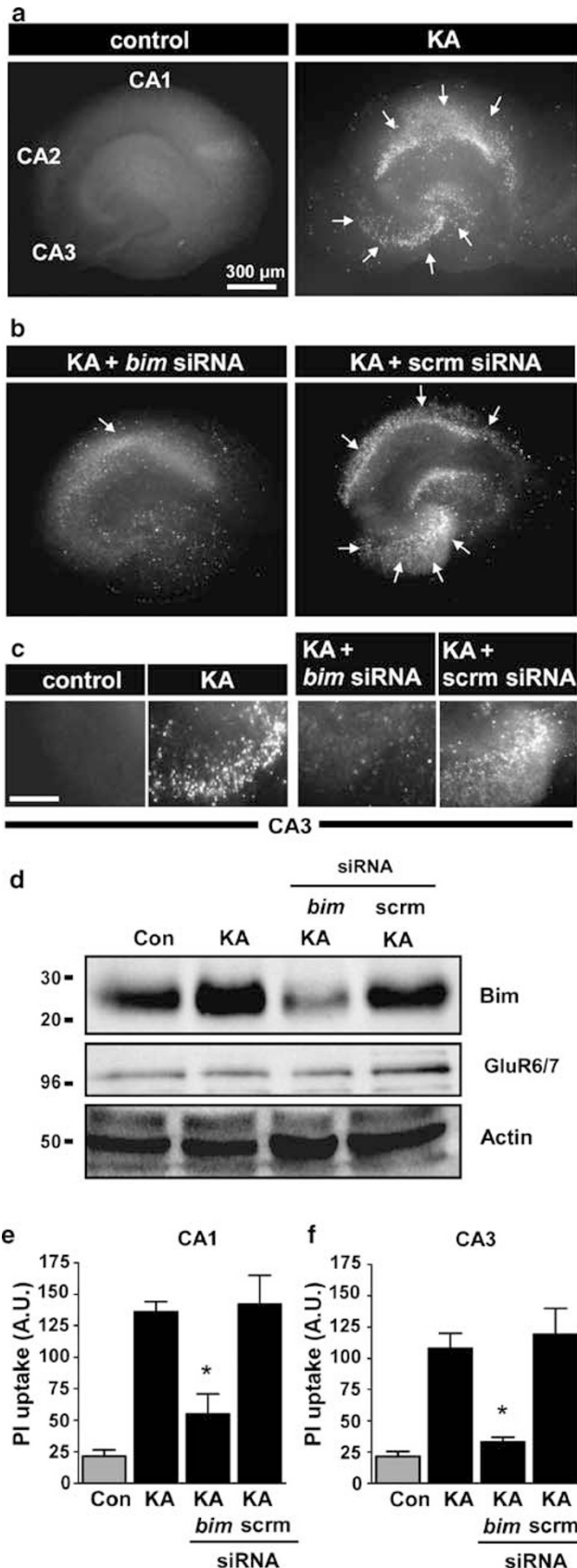


**Figure 5** Hippocampal but not neocortical seizure damage is reduced in *bim*<sup>-/-</sup> mice. (a, b) Representative photomicrographs (4 × lens) of Fluoro-Jade B staining within the ipsilateral hippocampus 72 h after *status epilepticus* in wild-type (wt) and *bim*<sup>-/-</sup> mice. Note the reduction in the numbers of damaged/dying cells within CA3 in *bim*<sup>-/-</sup> mice compared with that in wild-type animals. (c–f) Representative photomicrographs (40 × lens) of Fluoro-Jade B staining within the ipsilateral hippocampal CA3a and CA3b/c regions 72 h after *status epilepticus* in wild-type and *bim*<sup>-/-</sup> mice. Note the reduced numbers of Fluoro-Jade B-positive cells in *bim*<sup>-/-</sup> mice compared with wild-type animals. (g, h) Graphs quantifying the numbers of Fluoro-Jade B-stained cells in hippocampal CA3 and the neocortex for each genotype of mice. Data are derived from *n* = 6–10 per group. \**P* < 0.05. *ns*, not significant. (i, j) Representative photomicrographs (4 × lens) of Fluoro-Jade B staining within the ipsilateral neocortex 72 h after *status epilepticus* in wild-type and *bim*<sup>-/-</sup> mice



yet released 1 h after *status epilepticus* in this model, but is evident by 4 h.<sup>3</sup> These data extend our previous studies performed in rats subjected to focal-onset *status epilepticus* in which Bim protein was also found to be upregulated at 4 h.<sup>23</sup> Our data are also in agreement with findings of increased Bim levels after pilocarpine-induced *status epilepticus*.<sup>30</sup> However, our data contrast the report by Korhonen *et al.*,<sup>31</sup> who found that hippocampal Bim expression declined after *status epilepticus* induced by intracerebroventricular KA injection. The increase in hippocampal Bim protein that we detected is rather higher than would be expected from the relatively modest increase in *bim* mRNA levels. This may indicate that increased expression of Bim is a combination of transcriptional as well as posttranslational activation mechanisms. Consistent with this hypothesis, we observed the activation of transcription factors linked to *bim* induction (e.g., CHOP) as well as posttranslational activators of Bim (e.g., JNK). Both these events preceded the increase in Bim protein. As SP600125 blocked Bim induction, as well as CHOP after seizures, the JNK pathway may be most critical. However, it remains possible that other transcription factors and/or posttranslational regulators may also have a role in Bim regulation in *status epilepticus*. Indeed, seizure model data from rats previously linked FoxO1 to Bim induction.<sup>23</sup> Moreover, CHOP has been shown to trigger Bim expression in at least certain cell types after endoplasmic reticulum stress,<sup>15</sup> and endoplasmic reticulum stress is a feature of both seizure-induced neuronal death<sup>32</sup> and chronic human TLE.<sup>33</sup>

This study demonstrates that Bim has a causal role in the *status epilepticus*-induced cell death process because neurodegeneration was reduced in *bim*<sup>-/-</sup> mice. These are the first data showing that deficiency of a BH3-only protein can reduce seizure damage *in vivo*. Our analysis of damage was undertaken 3 days after *status epilepticus*, probably excluding an observation regarding the absence of Bim delaying rather than blocking cell death, as reported for Bim in other models.<sup>34</sup> Nevertheless, neurodegeneration after *status epilepticus* can continue for several weeks.<sup>35</sup> *bim* depletion by siRNA was also found to protect against hippocampal cell death after KA treatment *in vitro*. As Bim deficiency was not fully protective *in vivo*, it seems likely that other BH3-only proteins or other mechanisms are also involved in neuronal death after seizures in this model. Our data contrast findings by Theophilus *et al.*,<sup>36</sup> who reported that hippocampal damage was not different between wild-type and Bim-deficient mice

**Figure 6** Bim depletion by short interfering RNA reduces KA-induced neuronal death in hippocampal organotypic cultures. (a) Representative photomicrographs (4 × lens) show control and KA-treated cultures at 24 h stained with propidium iodide (PI). Note the significant cell death within hippocampal CA1 and CA3 (arrows). (b) Representative PI staining in KA-treated cultures at 24 h. Note, cell death is reduced in cultures transfected with short interfering RNA targeting *bim* (*bim* siRNA) compared with that in cultures treated with a scrambled sequence (scrm siRNA). (c) Representative PI staining in CA3 for each group. (d) Representative western blots (*n* = 3 per lane) showing that expression of Bim after KA treatment increases, and that *bim* siRNA reduces Bim protein levels. The blots below show that levels of the KA receptor were not altered by treatments, and probing for actin is provided as a control for protein loading. Data are derived from three independent experiments. (e, f) Graphs show quantification of cell death in CA1 and CA3 24 h after treatment. \**P* < 0.05 for comparison between cultures treated with KA plus *bim* siRNA compared with KA-treated cultures treated with scrambled siRNA. Graph data are from *n* = 3 per group.

after intra-hippocampal KA injection. The explanation for this discrepancy is unclear. However, Theofilas *et al.* used a model of direct intrahippocampal KA injection, in which dissociation of seizure effects *versus* direct KA toxicity is not possible. In contrast, our model uses KA to elicit *status epilepticus* from a site remote from the target hippocampus and we could confirm recruitment of the hippocampus in seizures using intracerebral recordings. Thus, hippocampal damage in the present model results from local glutamatergic and other mechanisms, not from direct toxic effects of KA on hippocampal cells. That said, we found that Bim reduction by siRNA was also neuroprotective *in vitro*, in which seizure-related injury is not dissociable from the direct toxic effects of KA. Theofilas *et al.* also did not report data on hippocampal CA3 damage comparing *bim*<sup>-/-</sup> and wild-type mice, nor did they report Bim expression in their model. As we observed that in locations in which Bim is not induced (i.e., in the neocortex) deficiency of Bim confers no protective advantage, this remains a possible explanation for the differences between the results from these two studies. Nevertheless, these data suggest that Bim is not always required for seizure-induced neuronal death. We emphasize the importance of interpreting our data within the context of the model used and caution in extrapolating findings to the human condition.

These studies may have implications for Bim involvement in other acute neurological insults featuring an excitotoxic component, such as ischemia. Indeed, ischemia induces Bim expression,<sup>37</sup> and neonatal hypoxia–ischemic injury-induced neuronal death in mice is reduced by loss of Bim.<sup>28</sup> Although the molecular mechanism of Bim-induced neuronal death was not a focus of our study, we previously showed that Bim binds to antiapoptotic Bcl-w *in vivo* after seizures in rats and mice.<sup>3,23</sup> However, other mechanisms of action are possible. Bim has been reported to contribute to the release of AIF in neurons,<sup>22</sup> and AIF mediates a component of seizure-induced neuronal death.<sup>4</sup>

This study complements findings on antiapoptotic Bcl-2 family proteins in seizure-induced neuronal death. Overexpression of Bcl-xL protects the hippocampus against seizure-like insults *in vivo*.<sup>7</sup> In our earlier report on Bcl-w using the same model applied presently, we found that Bcl-w was targeted by Bim during seizure-induced neuronal death and that Bcl-w deficiency led to significantly enhanced hippocampal damage from seizures.<sup>3</sup> However, *bcl-w*<sup>-/-</sup> mice showed earlier seizure onset than did wild-type animals, implying an endogenous function for that gene that, when disrupted, leads to higher seizure susceptibility.<sup>3</sup> We observed no seizure abnormalities in *bim*<sup>-/-</sup> mice, which is in agreement with EEG recordings in *bim*<sup>-/-</sup> mice after intrahippocampal KA.<sup>36</sup> This implies that basal Bim expressed in neurons may have limited roles in normal neuronal physiology. These observations emphasize the potential value of targeting certain proapoptotic BH3-only proteins.

The second finding of significance in this study was that Bim was downregulated in the less-damaged neocortex after *status epilepticus*. Furthermore, the transcriptional and posttranslational pathways associated with Bim induction in the hippocampus were not recruited in the neocortex. These data may provide evidence for seizure-induced tolerance mechanisms in the neocortex. Indeed, we showed earlier that

Bim expression is downregulated in the rat hippocampus after repeated brief, nonharmful electroshock seizures,<sup>23</sup> a model of epileptic tolerance. These findings may constitute the experimental correlate of human data showing lower Bim levels in brains from patients with intractable epilepsy.<sup>23</sup> Such adjustments to proapoptotic Bcl-2 family proteins have been reported elsewhere,<sup>38</sup> and may represent endogenous mechanisms to reduce vulnerability to seizure-induced neuronal death. The mechanism of Bim downregulation in the neocortex is currently unknown. The rapid rundown excludes a simple block on new mRNA production. Indeed, the half-life of Bim in neurons is estimated at 2.8 h,<sup>20</sup> and we found Bim levels were below 50% in samples 1 h after *status epilepticus*. More likely, Bim is degraded, for example, through ubiquitination, which is triggered by mitogen-activated protein kinases or other mediators.<sup>20</sup> An alternative mechanism may lie with protein kinase B/Akt.<sup>39</sup> We showed using a rat model that Akt is activated in the neocortex in response to *status epilepticus*, but when this is blocked, Bim upregulation occurs, resulting in increased neocortical cell death.<sup>5,23</sup> Finally, our *in vitro* data raise the intriguing possibility of intrinsic differences between hippocampal and cortical neurons in the importance of Bim for seizure- and excitotoxin-induced cell death.

In conclusion, this study shows a complex relationship between Bim expression, seizures and neuronal death *in vivo*, but provides further evidence that the Bcl-2 family of genes has a significant role in seizure-induced neuronal death. Bim is induced in a temporally compatible pattern with hippocampal neuronal death, and significant, although moderate, neuroprotection could be shown in its absence. As Bim expression is also regulated in the hippocampus from patients with intractable temporal lobe epilepsy<sup>23,33</sup>, the present data may be relevant not just for neuroprotection in the wake of *status epilepticus* but also in intractable epilepsy in which patients may be at risk of progressive damage over time to involved brain structures.

## Materials and Methods

***In vivo* model of focal-onset *status epilepticus* in mice.** Animal experiments were carried out in accordance with the principles of the European Communities Council Directive (86/609/EEC) and the National Institute of Health's *Guide for the Care and Use of Laboratory Animals*. Procedures were reviewed and approved by the research ethics committee of the Royal College of Surgeons in Ireland, under license from the Department of Health, Dublin, Ireland.

Studies were performed according to previously described techniques.<sup>25</sup> Mice (C57BL/6 adult male, 8–10-weeks old, 20–25 g) were obtained from Harlan, UK. *Bim* wild-type mice (*bim*<sup>+/+</sup>) and *bim* knockout (*bim*<sup>-/-</sup>) mice, originally generated on a mixed C57BL/6 × 129SV background using 129SV-derived ES cells, backcrossed for at least eight generations on a C57BL/6 genetic background have been described earlier.<sup>21</sup> Mice were anesthetized using isoflurane (3–5%) and maintained normothermic by means of a feedback-controlled heat blanket (Harvard Apparatus Ltd, Kent, UK). A catheter was inserted into the femoral vein for administration of an anticonvulsant. Mice were next placed in a stereotaxic frame and, after a midline scalp incision, three partial craniectomies were performed. The mice were then affixed with cortical electrodes (Bilaney Consultants Ltd, Sevenoaks, UK) to record surface EEG. Electrodes were placed above the dorsal hippocampus and a third was placed over the frontal cortex. EEG was recorded using a Grass Comet digital EEG (Medivent Ltd, Lucan, Ireland). For combined intrahippocampal with cortical recordings, additional mice were anesthetized and stereotaxically implanted with a twisted wire bipolar electrode (Bilaney Consultants Ltd, Sevenoaks, UK), into the dorsal CA3 subfield of the hippocampus, whereas cortical EEG was recorded by means of two skull-mounted recording electrodes (Bilaney Consultants Ltd) placed



over the frontal cortex and cerebellum and secured with dental cement. A guide cannula was affixed (coordinates from Bregma: AP = -0.94; L = -2.85 mm) and the entire skull assembly was fixed in place with dental cement. Anesthesia was then discontinued and freely moving mice were placed in a clear Perspex recording chamber. EEG recordings were commenced, and after establishing baseline EEG, an injection cannula was lowered through the guide cannula to 3.75 mm below the dura for microinjection of 0.3 µg KA (Ocean Produce International, Nova Scotia, Canada) in 0.2 µl phosphate-buffered saline (PBS) into the basolateral amygdala nucleus. Nonseizure control mice received the same volume of intra-amygdala vehicle. Forty minutes after microinjection of KA or vehicle, mice received intravenous lorazepam (6 mg/kg) and EEG was monitored for up to 1 h thereafter. Mice were killed 1, 2, 4, 6, 8, 24 or 72 h after lorazepam and were perfused with saline to remove intravascular blood components. Brains were either flash-frozen whole in 2-methylbutane at -30 °C for histopathology or the hippocampus and neocortex were microdissected and processed for mRNA and protein analysis, as described below.

**In vivo effect of JNK inhibitor SP600125.** Additional groups of control and seizure mice were instrumented for intracerebroventricular administration of vehicle or JNK inhibitor SP600125.<sup>25</sup> Briefly, mice were implanted with a second cannula ipsilateral to the side of KA injection. Coordinates from Bregma were as follows: AP = -0.3 mm, L = -1.0 mm and V = -2.0 mm. Mice received 1.75 µl infusions of either vehicle (25 % DMSO in PBS) or SP600125 (0.5 mM stock; resultant cerebrospinal fluid concentration approximating 25 µM) 15 min before KA and again 1 h after KA. A separate group of nonseizure control mice received vehicle into both ventricle and amygdala. Mice were killed 24 h later and the ipsilateral hippocampus was removed and processed for western blotting as described below.

**Genotyping.** Genotyping was performed according to previously described methods.<sup>21</sup> Genomic DNA was extracted from tail snips. A triple primer protocol was used to identify genotypes: primer 1, CATTCTCGTAAGTCCGAGTCT; primer 2, CTCAGTCCATTCATCAACAG; and primer 3, GTGCTAACTGAAACCAGATTA. The amplified fragments, detected by DNA agarose electrophoresis, were 400 bp for wild-type (*bim*<sup>+/+</sup>), 550 bp + 400 bp for heterozygote (*bim*<sup>+/-</sup>) and 550 bp only for knockout (*bim*<sup>-/-</sup>).

**In vitro models of seizure-like injury.** Organotypic hippocampal slice cultures were prepared and maintained as described earlier.<sup>27</sup> Briefly, 10-day-old C57BL/6 mice of either sex were decapitated, their brains removed and placed in dissection media containing Hanks Balanced Salt Solution (Gibco, Carlsbad, CA, USA), 20 mM Hepes (Gibco), 100 U/ml penicillin/streptomycin (Sigma-Aldrich, Dublin, Ireland) and 6.5 mg/ml D-glucose (Sigma-Aldrich). Hippocampi were then dissected and cut into 450 µm-thick sections. The slices were then transferred into fresh dissection media and were selected on the basis of the presence of intact hippocampal subfields (CA1, CA3 and the dentate gyrus). The slices were then transferred onto the porous (0.4 µm) membrane of a Millipore insert (Millipore, Cork, Ireland). These inserts were then placed into 24-well tissue culture plates, with each well containing 300 µl of culture medium consisting of 50% minimal essential medium (MEM) (Sigma-Aldrich), 25% horse serum (Gibco), 4 mM L-glutamine, 6 mg/ml D-glucose, 2% B27 and 50 U/ml penicillin/streptomycin. The slices were then incubated in a humidified chamber with 5% CO<sub>2</sub> at 35 °C. Cultures were maintained for up to 12 days and the medium was changed every 3–4 days. To model seizure-like injury, cultures were treated with KA (5 µM) (Sigma-Aldrich) for 24 h at 35 °C. Control slices were incubated with medium treated with vehicle. For RNA interference (RNAi) experiments, hippocampal cultures were transiently transfected with a mouse-specific pool of three target-specific 20–25 nt siRNAs to deplete *bim* (sc-29803, Santa Cruz Biotechnology, Santa Cruz, CA, USA). The siRNA duplexes were resuspended in 330 µl of RNase-free water at a stock concentration of 10 µM and transfections were performed for 24 h using a siRNA transfection reagent (sc-29528, Santa Cruz Biotechnology) with siRNA at a concentration of 0.8 µM in culture media. Control cultures were treated with a scrambled sequence that does not lead to a specific degradation of any known cellular mRNA (sc-37007, Santa Cruz Biotechnology). Cell death was assessed by propidium iodide (PI) uptake.<sup>27</sup> Briefly, PI (5 µg/ml) was introduced into cultures for 40 min and then washed out through medium change. Fluorescence from dead cells that take up the dye in the nucleus was visualized using a Hamamatsu Orca 285 camera (Micron-Optica, Ennisclorthy, Ireland) attached to a Nikon 2000 s epifluorescence microscope under 540–580/600–660 nm (red). Analysis of the optical density of PI staining was carried out using Image J (Micron-Optica; <http://rsb.info.nih.gov/ij/>). PI staining was determined for each subregion of the hippocampus as the

average of five field views of 1 µm<sup>2</sup>. Data were averaged from three similarly treated slices and at least three independent experiments were carried out for each condition.

For primary cortical cultures, wild-type or *bim*<sup>-/-</sup> mouse embryos (E16–E18) were isolated by hysterectomy and transferred to a dissection medium (PBS with 0.25% glucose and 0.3% BSA) on ice. The cerebral cortex from each embryo was isolated and then incubated with trypsin-EDTA (0.25%) at 37 °C for 15 min. The tissue was then dissociated in 5 ml of plating medium (MEM containing 5% fetal calf serum, 5% horse serum, 100 U/ml Pen/strep, 0.5 mM L-glutamine and 6% glucose). After dissociation, the neurons were pelleted by centrifugation. Media were aspirated and neurons were resuspended in fresh plating medium and plated at 7 × 10<sup>5</sup> cells per ml on polylysine-coated plates. Cells were incubated at 37 °C, 5% CO<sub>2</sub> in feeding media (NBM-embryonic containing 100 U/ml of Pen/Strep, 2% B27 and 0.5 mM L-glutamine and 1 µM cytosine arabinofuranoside). Media were changed every 2–3 days until day *in vitro* 6 (DIV 6) and cortical neurons were exposed to varying concentrations of KA (3–30 µM) on DIV 7. Cell death was assayed 24 h after treatments by incubation with Hoechst 33258 (1 µg/ml) for 10 min. Images were captured under a Nikon TE-2000 s epifluorescence microscope (Micro-optica, Dublin, Ireland) using a 20 × objective. The number of pyknotic nuclei was manually quantified and expressed as a percentage of total neuronal cells in a field. Each field contained 400–500 cells and each dose/data point was determined from three separate wells, each in triplicate.

**mRNA analysis.** Real-time quantitative PCR analysis of *bim* mRNA levels was undertaken. Primers were designed using Primer3 software (<http://frodo.wi.mit.edu>) and verified by BLAST (<http://blast.ncbi.nlm.nih.gov/Blast.cgi>): Forward, CAA CACAAACCCCAAGTCCT; Reverse, CATTTCGCAAAACACCTCCTT. One microgram total RNA from control (2 h) and seizure hippocampus (2–8 h) was used to generate cDNA by reverse transcription using the Superscript II Reverse Transcriptase enzyme (Invitrogen Corporation, Carlsbad, CA, USA). Quantitative real-time PCR was performed using a LightCycler 1.5 (Roche Diagnostics, Indianapolis, IN, USA) in combination with a QuantiTech SYBR Green PCR kit (Qiagen Ltd, Crawley, UK) as per the manufacturer's protocol, and 1.25 µM of primer pair was used. Data were analyzed by LightCycler 1.5 software with data normalized to the expression of β-actin.

**Western blot analysis.** Western blotting was performed as previously described.<sup>3,27</sup> Whole hippocampus, amygdala tissue cores<sup>3</sup> or pools of 3–4 organotypic slices were homogenized in buffer containing a protease inhibitor cocktail. After determining the total protein concentration, 20 µg samples were boiled in a gel-loading buffer and separated on 12–15% SDS-PAGE gels. Proteins were transferred to nitrocellulose membranes and incubated with the following antibodies: β-actin, CHOP (Santa Cruz Biotechnology), Bim (Stressgen, Victoria, BC, Canada), Bad, JNK, phospho-JNK, FoxO1, phospho-FoxO1, FoxO3 and phospho-FoxO3 (Cell signaling Technology, Beverly, MA, USA), Bcl-xL (BD Biosciences, Oxford, UK) and GluR6/7 (Millipore). Membranes were next incubated with horseradish peroxidase-conjugated secondary antibodies (Jackson Immuno-Research, Plymouth, PA, USA) and protein bands were visualized using Super-signal West Pico Chemiluminescent Substrate (Pierce, Rockford, IL, USA). Images were captured using a Fuji-film LAS-3000 (Fuji, Sheffield, UK), densitometry was performed using AlphaEaseFC4.0 software and data were expressed as change relative to control.

**Histopathology and immunohistochemistry.** Brains were sectioned at -20 °C on a Leica cryostat and 12 µm sections were collected at the level of dorsal hippocampus (AP from Bregma; -1.82 mm according to a mouse stereotaxic atlas.<sup>40</sup> Neuronal damage was assessed using Fluoro-Jade B (FJB) as previously described.<sup>25</sup> Briefly, sections were air-dried and postfixed in 10% formalin. Next, sections were hydrated through graded alcohols, rinsed in distilled water and transferred to 0.006% potassium permanganate solution for 15 min with gentle shaking. Sections were rinsed again and transferred to FJB solution (0.001% in 0.1% acetic acid) (Chemicon Europe Ltd, Chandlers Ford, UK). After staining, sections were rinsed again, dried, cleared and mounted in DPX (Sigma-Aldrich). Hippocampal FJB-positive counts were the average of two adjacent sections for the CA3 subfield. Counts of FJB-positive cells in the neocortex were the average sum of ten 40 × lens fields from two adjacent sections within the ectorhinal, perirhinal and piriform cortices. Counts were determined by an observer blinded to the experimental treatment.

For Bim immunohistochemistry, sections were fixed and permeabilized, blocked in goat serum and then incubated overnight with anti-Bim, followed by incubation

with goat anti-rabbit AlexaFluor568 (Molecular Probes, Eugene, OR, USA). Next, sections were stained for DNA fragmentation using a fluorescein-based TUNEL kit (Promega US, Madison, WI, USA) as previously described.<sup>3,5</sup> Sections were examined using a Nikon 2000 S epifluorescence microscope under Ex/Em wavelengths of 472/520 nm (green) and 540–580/600 to 660 nm (red) using a Hamamatsu Orca 285 camera.

For analysis of the naive brains of wild-type compared with *bim*<sup>-/-</sup> mice, coronal mouse brain sections were immunostained with antibodies against NeuN (Millipore), followed by goat anti-mouse AlexaFluor568 (Molecular Probes), and were visualized as above. Counts of NeuN-stained hippocampal CA1, CA2 and CA3 from naive wild-type and *bim*<sup>-/-</sup> mice were the mean from two adjacent sections at the level of the dorsal hippocampus.

**Statistical analysis.** Data are presented as mean  $\pm$  S.E.M. Comparison of data was performed using one-way analysis of variance (ANOVA), followed by *post hoc* Fisher's PLSD test or Student's *t*-test. Significance was accepted at  $P < 0.05$ .

**Acknowledgements.** We thank Philippe Bouillet for the original generation of Bim-deficient mice and Aurelien Caballero, Michelle Ashley and Aine Murphy for technical support. This study was funded by the Health Research Board Ireland (RP/2005/24 to DH, PD/2005/35, RP/2008/69 to BM), Science Foundation Ireland (07/SK/B1243A to BM, 08/IN/1/B1875 to DH), Wellcome Trust (GR076576 to DH), Irish Research Council for Science Engineering and Technology (to TE), Marie Curie ToK FP-14499 and by the National Institutes of Health/National Institute of Neurological Disorders and Stroke (NS39016, NS47622 to RS). Additional support was provided to AS from NHMRC (Canberra; programs # 461221), from the Leukemia and Lymphoma Society (SCOR grant # 7015), the NIH (CA043540-18 and CA80188-6), the JDRF/NHMRC and from the Charles and Sylvia Viertel Charitable Foundation (PB).

- Engel T, Henshall DC. Apoptosis, Bcl-2 family proteins and caspases: the ABCs of seizure-damage and epileptogenesis? *Int J Physiol Pathophysiol Pharmacol* 2009; **1**: 97–115.
- Youle RJ, Strasser A. The BCL-2 protein family: opposing activities that mediate cell death. *Nat Rev Mol Cell Biol* 2008; **9**: 47–59.
- Murphy B, Dunleavy M, Shinoda S, Schindler C, Meller R, Bellver-Estelles C *et al*. Bcl-w protects hippocampus during experimental status epilepticus. *Am J Pathol* 2007; **171**: 1258–1268.
- Cheung EC, Melanson-Drapeau L, Cregan SP, Vanderluit JL, Ferguson KL, McIntosh WC *et al*. Apoptosis-inducing factor is a key factor in neuronal cell death propagated by BAX-dependent and BAX-independent mechanisms. *J Neurosci* 2005; **25**: 1324–1334.
- Henshall DC, Araki T, Schindler CK, Lan J-Q, Tiekoter K, Taki W *et al*. Activation of Bcl-2-associated death protein and counter-response of Akt within cell populations during seizure-induced neuronal death. *J Neurosci* 2002; **22**: 8458–8465.
- Xiang H, Kinoshita Y, Knudson CM, Korsmeyer SJ, Schwartzkroin PA, Morrison RS. Bax involvement in p53-mediated neuronal cell death. *J Neurosci* 1998; **18**: 1363–1373.
- Ju KL, Manley NC, Sapolsky RM. Anti-apoptotic therapy with a Tat fusion protein protects against excitotoxic insults *in vitro* and *in vivo*. *Exp Neurol* 2008; **210**: 602–607.
- Yan C, Chen J, Chen D, Minami M, Pei W, Yin XM *et al*. Overexpression of the cell death suppressor Bcl-w in ischemic brain: implications for a neuroprotective role via the mitochondrial pathway. *J Cereb Blood Flow Metab* 2000; **20**: 620–630.
- Cao G, Xing J, Xiao X, Liou AK, Gao Y, Yin XM *et al*. Critical role of calpain I in mitochondrial release of apoptosis-inducing factor in ischemic neuronal injury. *J Neurosci* 2007; **27**: 9278–9293.
- O'Connor L, Strasser A, O'Reilly LA, Hausmann G, Adams JM, Cory S *et al*. Bim: a novel member of the Bcl-2 family that promotes apoptosis. *EMBO J* 1998; **17**: 384–395.
- O'Reilly LA, Cullen L, Visvader J, Lindeman GJ, Print C, Bath ML *et al*. The proapoptotic BH3-only protein bim is expressed in hematopoietic, epithelial, neuronal, and germ cells. *Am J Pathol* 2000; **157**: 449–461.
- Dijkers PF, Medema RH, Lammers JW, Koenderman L, Coffey PJ. Expression of the proapoptotic Bcl-2 family member Bim is regulated by the forkhead transcription factor FKHR-L1. *Curr Biol* 2000; **10**: 1201–1204.
- Stahl M, Dijkers PF, Kops GJ, Lens SM, Coffey PJ, Burgering BM *et al*. The forkhead transcription factor FoxO regulates transcription of p27Kip1 and Bim in response to IL-2. *J Immunol* 2002; **168**: 5024–5031.
- Whitfield J, Neame SJ, Paquet L, Bernard O, Ham J. Dominant-negative c-Jun promotes neuronal survival by reducing BIM expression and inhibiting mitochondrial cytochrome c release. *Neuron* 2001; **29**: 629–643.
- Puthalakath H, O'Reilly LA, Gunn P, Lee L, Kelly PN, Huntington ND *et al*. ER stress triggers apoptosis by activating BH3-only protein Bim. *Cell* 2007; **129**: 1337–1349.
- Putcha GV, Le S, Frank S, Besirli CG, Clark K, Chu B *et al*. JNK-mediated BIM phosphorylation potentiates BAX-dependent apoptosis. *Neuron* 2003; **38**: 899–914.
- Becker EB, Howell J, Kodama Y, Barker PA, Bonni A. Characterization of the c-Jun N-terminal kinase-BimEL signaling pathway in neuronal apoptosis. *J Neurosci* 2004; **24**: 8762–8770.
- Harada H, Quearry B, Ruiz-Vela A, Korsmeyer SJ. Survival factor-induced extracellular signal-regulated kinase phosphorylates BIM, inhibiting its association with BAX and proapoptotic activity. *Proc Natl Acad Sci USA* 2004; **101**: 15313–15317.
- Biswas SC, Greene LA. Nerve growth factor (NGF) down-regulates the Bcl-2 homology 3 (BH3) domain-only protein Bim and suppresses its proapoptotic activity by phosphorylation. *J Biol Chem* 2002; **277**: 49511–49516.
- Meller R, Cameron JA, Torrey DJ, Clayton CE, Ordonez AN, Henshall DC *et al*. Rapid degradation of Bim by the ubiquitin-proteasome pathway mediates short-term ischemic tolerance in cultured neurons. *J Biol Chem* 2006; **81**: 7429–7436.
- Bouillet P, Metcalf D, Huang DC, Tarlinton DM, Kay TW, Kontgen F *et al*. Proapoptotic Bcl-2 relative Bim required for certain apoptotic responses, leukocyte homeostasis, and to preclude autoimmunity. *Science* 1999; **286**: 1735–1738.
- Liou AK, Zhou Z, Pei W, Lim TM, Yin XM, Chen J. BimEL up-regulation potentiates AIF translocation and cell death in response to MPTP. *FASEB J* 2005; **19**: 1350–1352.
- Shinoda S, Schindler CK, Meller R, So NK, Araki T, Yamamoto A *et al*. Bim regulation may determine hippocampal vulnerability after injurious seizures and in temporal lobe epilepsy. *J Clin Invest* 2004; **113**: 1059–1068.
- Shinoda S, Araki T, Lan JQ, Schindler CK, Simon RP, Taki W *et al*. Development of a model of seizure-induced hippocampal injury with features of programmed cell death in the BALB/c mouse. *J Neurosci Res* 2004; **76**: 121–128.
- Mouri G, Jimenez-Mateos E, Engel T, Dunleavy M, Hatazaki S, Paucard A *et al*. Unilateral hippocampal CA3-predominant damage and short latency epileptogenesis after intra-amygdala microinjection of kainic acid in mice. *Brain Res* 2008; **1213**: 140–151.
- Bennett BL, Sasaki DT, Murray BW, O'Leary EC, Sakata ST, Xu W *et al*. SP600125, an anthracycline inhibitor of Jun N-terminal kinase. *Proc Natl Acad Sci USA* 2001; **98**: 13681–13686.
- Murphy N, Bonner HP, Ward MW, Murphy BM, Prehn JH, Henshall DC. Depletion of 14-3-3 zeta elicits endoplasmic reticulum stress and cell death, and increases vulnerability to kainate-induced injury in mouse hippocampal cultures. *J Neurochem* 2008; **106**: 978–988.
- Ness JM, Harvey CA, Strasser A, Bouillet P, Klocke BJ, Roth KA. Selective involvement of BH3-only Bcl-2 family members Bim and Bad in neonatal hypoxia-ischemia. *Brain Res* 2006; **1099**: 150–159.
- Hetz C, Thieleen P, Fisher J, Pasinelli P, Brown RH, Korsmeyer S *et al*. The proapoptotic BCL-2 family member BIM mediates mitonuclear loss in a model of amyotrophic lateral sclerosis. *Cell Death Differ* 2007; **14**: 1386–1389.
- Yang J, Huang Y, Yu X, Sun H, Li Y, Deng Y. Erythropoietin preconditioning suppresses neuronal death following status epilepticus in rats. *Acta Neurobiol Exp (Wars)* 2007; **67**: 141–148.
- Korhonen L, Belluardo N, Mudo G, Lindholm D. Increase in Bcl-2 phosphorylation and reduced levels of BH3-only Bcl-2 family proteins in kainic acid-mediated neuronal death in the rat brain. *Eur J Neurosci* 2003; **18**: 1121–1134.
- Sokka AL, Putkonen N, Mudo G, Pryazhnikov E, Reijonen S, Khiroug L *et al*. Endoplasmic reticulum stress inhibition protects against excitotoxic neuronal injury in the rat brain. *J Neurosci* 2007; **27**: 901–908.
- Yamamoto A, Murphy N, Schindler CK, So NK, Stohr S, Taki W *et al*. Endoplasmic reticulum stress and apoptosis signaling in human temporal lobe epilepsy. *J Neuropathol Exp Neurol* 2006; **65**: 217–225.
- Putcha GV, Moulder KL, Golden JP, Bouillet P, Adams JA, Strasser A *et al*. Induction of BIM, a proapoptotic BH3-only BCL-2 family member, is critical for neuronal apoptosis. *Neuron* 2001; **29**: 615–628.
- Nairismagi J, Grohn OH, Kettunen MI, Nissinen J, Kauppinen RA, Pitkanen A. Progression of brain damage after status epilepticus and its association with epileptogenesis: a quantitative MRI study in a rat model of temporal lobe epilepsy. *Epilepsia* 2004; **45**: 1024–1034.
- Theofilas P, Bedner P, Huttman K, Theis M, Steinhauser C, Frank S. The proapoptotic BCL-2 homology domain 3-only protein Bim is not critical for acute excitotoxic cell death. *J Neuropathol Exp Neurol* 2009; **68**: 102–110.
- Inta I, Paxian S, Maegele I, Zhang W, Pizzi M, Spano P *et al*. Bim and Noxa are candidates to mediate the deleterious effect of the NF-kappa B subunit RelA in cerebral ischemia. *J Neurosci* 2006; **26**: 12896–12903.
- Kondratyev A, Sahibzada N, Gale K. Electroconvulsive shock exposure prevents neuronal apoptosis after kainic acid-evoked status epilepticus. *Brain Res Mol Brain Res* 2001; **91**: 1–13.
- Qi XJ, Wilder GM, Howe PH. Evidence that Ser87 of BimEL is phosphorylated by Akt and regulates BimEL apoptotic function. *J Biol Chem* 2006; **281**: 813–823.
- Franklin KBJ, Paxinos P. *The Mouse Brain in Stereotaxic Coordinates*. Academic Press, Inc: San Diego, 1997.

Supplementary Information accompanies the paper on Cell Death and Differentiation website (<http://www.nature.com/cdd>)